frontiers in Marine Science

ORIGINAL RESEARCH
published: 16 April 2020
doi: 10.3389/fmars.2020.00190

Geomorphometric Seabed Classification and Potential Megahabitat Distribution in the Amazon Continental Margin

Ana Carolina Lavagnino[1], Alex Cardoso Bastos[1], Gilberto Menezes Amado Filho[2†], Fernando Coreixas de Moraes[2], Lais Silva Araujo[3] and Rodrigo Leão de Moura[3]*

[1] Marine Geoscience Laboratory, Departamento de Oceanografia, Universidade Federal do Espírito Santo, Vitória, Brazil, [2] Instituto de Pesquisas Jardim Botânico do Rio de Janeiro, Rio de Janeiro, Brazil, [3] Instituto de Biologia and SAGE-COPPE, Universidade Federal do Rio de Janeiro, Rio de Janeiro, Brazil

OPEN ACCESS

Edited by:
Vincent Lecours, University of Florida, United States

Reviewed by:
Ian David Tuck, National Institute of Water and Atmospheric Research (NIWA), New Zealand
Fantina Madricardo, Italian National Research Council, Italy

***Correspondence:**
Alex Cardoso Bastos
alex.bastos@ufes.br

† Deceased

Specialty section:
This article was submitted to Deep-Sea Environments and Ecology, a section of the journal Frontiers in Marine Science

Received: *12 June 2019*
Accepted: *11 March 2020*
Published: *16 April 2020*

Citation:
Lavagnino AC, Bastos AC, Amado Filho GM, de Moraes FC, Araujo LS and de Moura RL (2020) Geomorphometric Seabed Classification and Potential Megahabitat Distribution in the Amazon Continental Margin. Front. Mar. Sci. 7:190. doi: 10.3389/fmars.2020.00190

The geomorphometry of the northeast portion of the Amazon Shelf, along the Brazilian Equatorial Margin (BEM), off the Amazonas River mouth, was analyzed using the Benthic Terrain Modeler, a spatial analysis technique that defines physical megahabitat classes based on seafloor relief heterogeneities. A compilation of bathymetric data was used to explore a regional level model, and novel high-resolution multibeam data were used to detail specific portions of the region, with emphasis on shelf–slope transitions and shelf-edge reefs. The analyses revealed a complex mosaic of benthic megahabitats that are associated to the shelf's morphology, distance offshore, and sediment discharge and transport. The massive and continuous terrigenous sediment input is associated to a smooth muddy deposit along the inner and mid shelf (Regular Continental Shelf megahabitat). The portions of the shelf that are less influenced by riverine sediment accumulation are rougher and characterized by either sand (Irregular Sand Continental Shelf megahabitat) or carbonate-dominated bottom (Irregular Reef Continental Shelf megahabitat). The most notable difference in terms of morphometric analysis and megahabitats can be observed along the outer shelf and shelf break. The shelf–slope transition megahabitat is marked by ridges in the shelf break and by a more acute depth gradient that forms a distinct outer shelf edge. Three different alongshore sectors were explored in order to describe the heterogeneous megahabitat mosaic in terms of slope and bottom morphology. The western-most sector (S3) is remarkable due to an indistinct separation between ridges and the outer shelf edge, as well as for presenting reefs with up to 20 m high, between 110- and 210-m water depths. The central sector (S2) presents no shelf break and lacks ridges, a feature that seems associated with the long-term sediment accumulation associated to the Amazon Fan. The southern-most sector (S1) does not present an outer shelf edge, only ridges, and presents a number of channels incised in the shelf, comprising an erosive area with sediment bypass across the shelf, and carbonate sedimentation. The continental slope is a vastly diverse domain

that may be further divided into a Featured Slope megahabitat with numerous canyons and ravines and a vast area that lacks such features, including a Shallow Gentle Slope megahabitat (<2,000-m water depth), a Steep Slope megahabitat, and a Deep Gentle Slope megahabitat. Our results confirm the usefulness of geomorphometric analyses to define benthic megahabitats and can be used as a starting point in a much-needed marine spatial planning process for the area.

Keywords: Benthic Terrain Modeler, benthic megahabitats, mesophotic reefs, drowned reefs, shelf-edge reefs

INTRODUCTION

The Brazilian Equatorial Margin (BEM) is the widest portion of the Brazilian continental margin and comprises, among others, the Foz do Amazonas Basin, with approximately 360,000 km^2 (Brandão and Feijó, 1994; Silva et al., 1999; Figueiredo et al., 2007). Here, we refer to this part of the BEM as the Amazon Continental Margin (ACM) (Cruz et al., 2019). The modern set of this margin was established at 2.5 Ma (early-Pleistocene) and evolved based on the reshape of the Amazon River due to the Andean uplift event during the Miocene (∼10 Ma) (Hoorn et al., 1995; Campbell, 2005; Figueiredo et al., 2009; Gorini et al., 2014). This event, progressively, gave away the predominance of a mixed and carbonate platform (Neogene Amapá carbonates) to a siliciclastic-dominated shelf, contributing to the development of the Amazon Fan (Milliman et al., 1975; Brandão and Feijó, 1994; Gorini et al., 2014). Cruz et al. (2019) show that mixed carbonate–siliciclastic sedimentation change spatially during the Neogene. An aggrading mixed shelf predominated across the entire Foz do Amazonas shelf during 24 and 8 Ma, with carbonates production giving away to siliciclastic sedimentation along the SE and Central shelves. Carbonate sedimentation was restricted to the NW shelf between 8 and 5.5 Ma. Continuous terrigenous sediment input from the Amazon river progressively buried the inner shelf carbonates, and carbonate sedimentation occurred in the NW outer shelf until 3.7 Ma (Cruz et al., 2019). In addition, low stand sea level during the Miocene was responsible for exposing, karstifying, and eroding carbonate deposits. Later on, from Mid-Pleistocene to Holocene, progradation produced a steeper slope prone to failure. Gravitational tectonics was responsible for mass wasting events, forming large megaslides, or mass-transport complexes that mobilized kilometer-thick deposits, extending for thousands of kilometers in the Amazon Fan (Reis et al., 2016).

Sedimentation along the ACM is highly influenced by the Amazon River, which is responsible for approximately 20% of the global riverine discharge to the ocean (Coles et al., 2013) and a sediment discharge of approximately 10 billion tons per year, developing a fine-grained submerged delta over an area of 3.3×10^5 km^2 (Meade et al., 1979; Kuehl et al., 1986; Nittrouer et al., 1986; Nittrouer and DeMaster, 1996). The Amazon River plume is superficial (25-m maximum depth) and driven by seasonal winds and by the North Brazilian Current (NBC), which flows northwestward into the Caribbean and retroflects eastward during September and October (Nittrouer and DeMaster, 1996). The main depocenter is largely driven by the NBC flow and occurs northwestward of the Amazon River mouth, off Amapá state. This plume and sediment dispersion dynamics is typically interglacial (highstand sea level) (Milliman et al., 1975, 1982; Nittrouer and DeMaster, 1986). During glacial (lowstand), sediment load bypasses the shelf break and is transported to the deep sea through various canyons and channels (Damuth and Fairbridge, 1970; Damuth and Kumar, 1975; Milliman et al., 1975; Damuth and Flood, 1984; Damuth et al., 1988) and may favor the active growth of biogenic carbonate structures on the outer shelf (Barreto et al., 1975; Milliman and Barretto, 1975a,b; Kumar et al., 1977; Moura et al., 2016).

The ACM is a promising area for the oil and gas industry, as part of the "Deep Water Golden Triangle" in the Atlantic Ocean (Brazil, Gulf of Mexico, and West Africa). These geologically similar margins comprise large accumulations of oil with high commercial value (Milani et al., 2001). More than a hundred exploratory blocks have been auctioned by Brazil since 2012, but environmental licensing is still a matter of discussion and concern (e.g., Francini-Filho et al., 2018), largely due to the recently mapped reef system off the Amazon mouth (Cordeiro et al., 2015; Moura et al., 2016).

Since the 1950s, there has been a vast amount of survey effort to characterize the stratigraphy and sediment dynamics of this margin, including the continental shelf (Milliman et al., 1975; Nittrouer et al., 1996) and slope (Reis et al., 2010; Silva et al., 2010; Gorini et al., 2014). However, a regional analysis of the geomorphology within the shelf–slope–rise transition was still lacking. Besides being relevant to understand the distribution of distinct seabed sedimentary features, such as an improved characterization of the benthic habitat mosaic off the Amazon mouth is an essential component for the development of an adequate marine spatial planning framework.

Considering the expansion of the oil and gas industry in the ACM, the occurrence of mesophotic reefs along the shelf and shelf break (Moura et al., 2016), and even the overestimated size of the "Great Amazon reefs" by Francini-Filho et al. (2018), a quantitative terrain characterization is a powerful tool to map potential benthic habitats based on their morphology (Lecours et al., 2016) and to set the stage for marine spatial planning (e.g., Moura et al., 2013). Herein, a quantitative terrain characterization is used to map potential benthic habitats based on their morphology. The objectives of this contribution are (i) to define the potential megahabitats along the equatorial/ACM; (ii) to investigate if spatial changes in geomorphometric patterns along the continental shelf and slope can be used as a proxy for habitats distribution; and

(iii) discuss the presence and potential formation of shelf-edge reefs.

MATERIALS AND METHODS

The ACM is located along the so-called BEM. A general bathymetric map of the study area is shown in **Figure 1**, with the three defined sectors, based on Moura et al. (2016) and Cruz et al. (2019), which were used to describe the changes in seafloor morphology and habitat distribution.

Bathymetric Data Set

The geomorphometric analyses were based on the Benthic Terrain Model (Walbridge et al., 2018), a modeling tool that indicates the potential occurrence of distinct habitats in terms of relief heterogeneity. A regional model was produced with the database from the Diretoria de Hidrografia e Navegação, Marinha do Brasil (LEPLAC Project). This bathymetric database is a compilation from seismic, single beam, multibeam, and remote sensing data acquired from GEODAS (NOAA Geophysical Data System), GEBCO (General Bathymetric Chart of the Oceans from International Hydrographic Organization and the Intergovernmental Oceanographic Commission, UNESCO), PETROBRAS, and ANP (Brazil's National Petroleum Agency). Data from STRM30_Plus V 7.0 (NASA Shuttle Radar Topography Mission) were used to fill regions lacking *in situ* data. Data validation was carried out by a cross-check verification considering control lines as references, using an Oasis Montaj tool, LevTie Line/Intersections and Rangrid GX/Geosoft. Minimum curvature and a cell size of 1,500 m were employed with Equatorial Mercator Projection and the WGS1984 Datum. Raw xyz data were interpolated using ArcGIS IDW method, originating a 2.5-km grid. Although the most used global dataset is GEBCO_2014, with 30-arc-second grids (900-m resolution), we used the LEPLAC project dataset, with 2-km grid but with comparatively greater accuracy at the regional level. We will refer to this regional bathymetric model as Leplac-DTM.

A detailed multibeam dataset was acquired on July 2017 during an oceanographic cruise with the M/V Alucia, using a Reson 7160 echosounder operating at a nominal frequency of 44 kHz. Backscatter data were not recorded. The survey aimed to detail morphological transitions in shelf–slope areas (**Figure 1**). Data were processed with CARIS HIPS and SIPS software to remove noise and adjust for sound velocity in the water column. Multibeam mosaics were built with a 40-m cell grid size and covered three different sectors of the continental slope. A detailed shelf-edge mosaic with 5-m cell grid size was produced for Sector 3, aiming to detail its reef structures.

Seabed Classes

The Leplac-DTM grid, along with its derivate slope and Bathymetric Position Index (BPI), was used to produce the morphometric analysis with the ArcGIS toolbox Benthic Terrain Modeler 3.0 (BTM), a suite of spatial analysis scripts for seabed classification (Walbridge et al., 2018).

Bathymetric Position Index evaluates elevation differences between a focal point and the mean elevation of its surrounding cells in an annulus, a ring shape bounded by two concentric circles that allow for the exclusion of immediately adjacent cells for measuring mean surrounding elevation (Lundblad et al., 2006; Walbridge et al., 2018). The outer radius multiplied by data resolution defines the scale factor, and the most suitable factor for the analysis is defined by trial and error (Erdey-Heydorn, 2008). Intrinsically scale dependent, BPI differentiates benthic features in both fine and broad scales. For example, at a small BPI neighborhood, a large valley would appear as a flat plain, whereas at a scale of several kilometers, the same area will look like a deep canyon. Combining BPI at fine and broad scales allows for the distinction of a variety of nested features. Positive cell values (greater than surrounding cells' mean) define high elevation areas (crests), negative values define low elevation areas (depressions), and near-zero or equal-to-zero values define flat areas (Weiss, 2001).

As spatial data tend to be auto correlated, the raw BPI has to be standardized to allow classification at almost any scale (Lundblad et al., 2006). The fine scale grid was generated with a scale factor of 5,000, and a broad scale grid was generated with a scale factor of 15,000. These scale factors were chosen on the basis that small seascape features are, on average, 5,000 m across. This is based on thorough observation of the bathymetry prior to BPI calculation.

The final step in the BTM analysis is related to the definition of a dictionary that categorizes the bathymetric BPI and the slope grid into user-defined classes that work within a lower and upper bound of grid units designated by the user (**Table 1**). Negative values mean below the standard deviation, whereas positive values mean above it. For example, in order to classify features such as depressions, the upper bound is set as negative values, whereas to classify positive features (e.g., crests), the lower bound is set as a positive value. An angle threshold of 0.1 was set for the classification of the slope (most of the shelf presents smaller values), with steep and gentle gradients falling above and below this threshold, respectively. In terms of depth, the continental shelf was divided into inner shelf (<40-m depth), mid shelf (40–60 m), outer shelf (60–100 m), and outer shelf edge (100–300 m).

Twelve seabed classes (**Table 1**) were defined based on depth (four classes), slope (two classes), and BPI (six classes). Classes based on depth include inner shelf (<40-m water depth), mid shelf (40–60 m), outer shelf (60–100 m), and outer shelf edge (100- to 300-m water depth). Classes based on slope are Gentle Slope (<0.1°) and Steep Slope (>0.1°). Classes based on BPI include Ridge 1 (crest on broad scales and a plateau where the gradient becomes less gentle), Ridge 2 (crest on both broad and fine scale, evidencing the shelf break or depression edges where the gradient is about to get steeper), Edges (crests on fine scale, associated with depression edges), Depression 1 (depression on both broad and fine scales and representing an axial incision associated with the thalweg of broad scale depressions), Depression 2 (axial incision associated with the thalweg of fine scale depressions), and Flanks (depressions on broad scale, related to depression's walls).

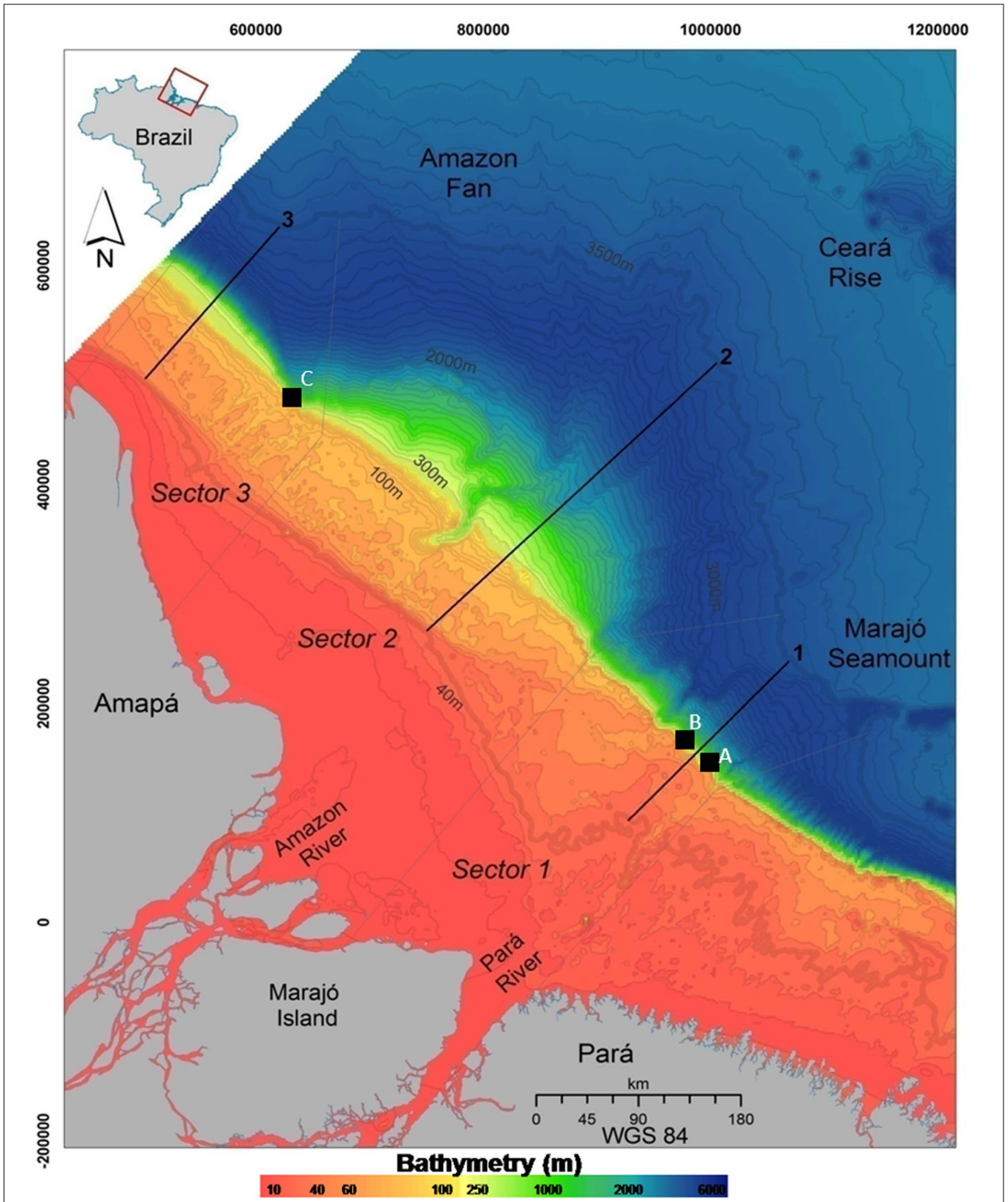

FIGURE 1 | The Brazilian Equatorial Margin (BEM) and the three sectors used in our geomorphometric descriptions. Gray dashed lines are sectors' borders, and black lines correspond to the longitudinal profiles within each sector (from 40- to 3,500-m water depth, thicker isobaths). Isobaths are spaced at each 10 m (up to 300-m water depth) or 100 m (deeper than 300 m). Black squares indicate the location of Multibeam data acquisition. **(A–C)** define the 2017 multibeam survey areas along the shelf edge.

TABLE 1 | BTM dictionary.

	Broad BPI		Fine BPI		Slope		Depth	
	Lower	Upper	Lower	Upper	Lower	Upper	Lower	Upper
(1). Inner shelf	−40	40	−40	40			−40	
(2). Mid shelf	−40	40	−40	40			−60	−40
(3). Outer shelf	−40	40	−40	40			−100	−60
(4). Outer shelf edge	−40	40	−40	40		0.1	−300	
(5). Ridge 1	40		40					
(6). Ridge 2	40		−40	40				
(7). Edges	−40	40	40					
(8). Depression 1		−40		−40				
(9). Flank		−40						
(10). Depression 2				−40				
(11). Gentle slope	−40	40	−40	40		0.1		
(12). Steep slope	−40	40	−40	40	0.1			

Seabed classes were categorized into BPI on both broad and fine scale, slope, and depth using a lower and upper bound. Forty grid units were used, and missing value indicates that the bound is not applicable to the seabed class.

A complementary Aspect Analysis was also carried out in order to analyze the mean orientation of the isobaths. This analysis is also derived from the bathymetric grid and allows for the identification of the downslope direction of the maximum rate of change from each cell to its neighbors, which corresponds to the dipping direction.

Sediment facies were compiled from Dutra's (2018) dataset (based mainly in Kuehl et al., 1996; Moura et al., 2016) and spatially combined in the GIS to produce physical megahabitat classes or seascapes along the ACM.

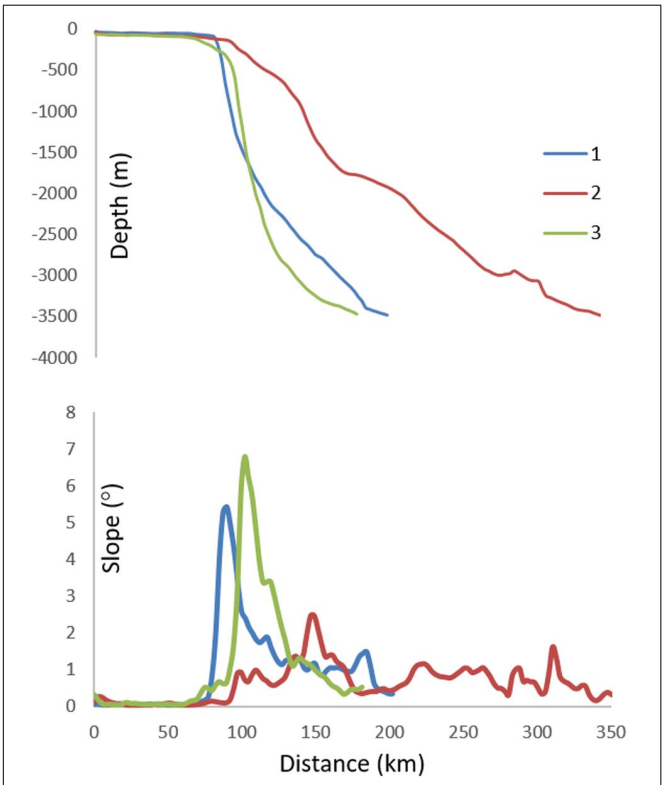

FIGURE 2 | Longitudinal geomorphological profiles from 40- to 3,500-m water depth for each sector (top graph) and corresponding slopes (bottom graph). Sector S1 breaks at approximately 100-m water depth and presents a concave curvature. Sector S2 has no defined break and a convex curvature, and sector S3 breaks at approximately 300-m water depth and shows a sigmoidal curvature.

Shelf–Slope Transitional Features

Features along the transition between the continental shelf and the slope were explored with the Leplac-DTM database and with our primary multibeam data. The Leplac-DTM was used to map individual depressions (canyons and/or incision-like features) on the slope. Classes Depression 1 and Depression 2 were used to set the beginning and the ending of depression features, and isobaths were used to track the axial incisions. Depression metrics were measured using ArcMap 10.1 toolbox and included length (m), sinuosity (length/straight length), area (km^2), minimum depth (m) where canyons start, maximum depth (m) where canyons end, and slope mean (°), this latter a gradient measurement at the canyon thalweg. Slope depressions were classified according to Harris and Whiteway (2011), assuming that canyons are depressions with at least 1000-m depth range, 100-m incision, and heads not deeper than 4,000-m water depth. Canyons can also be categorized as shelf incises or slope-confined canyons. If the feature does not fall within canyon metrics, it was described as a slope-confined depression.

RESULTS

The morphological profiles (**Figure 2**) show the distinct morphological characteristics among the three sectors. Sectors 1 and 3 have an abrupt and well-defined shelf breakpoint, whereas Sector S2 is smoother and lacks a clear shelf breakpoint (**Figure 2**). The distinction between S1 and S3 is related to the depth of the continental shelf break, at 100- and 300-m depth,

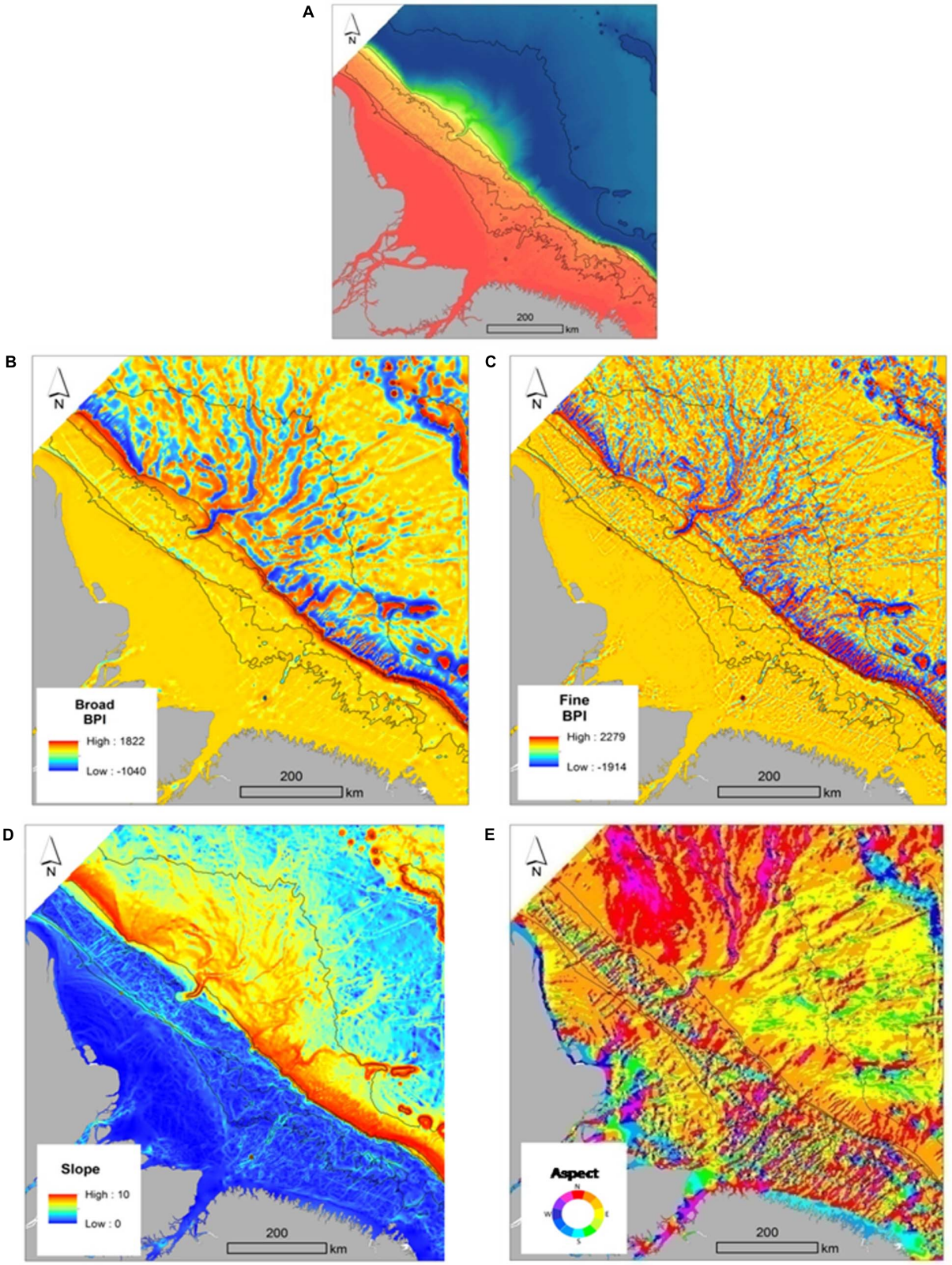

FIGURE 3 | Bathimetric grid **(A)**, Benthic Terrain Model results **(B–D)** and Aspect Grid **(E)**. Inserts **(B)** and **(C)** show the broad and fine BPI, respectively (standardized). Black lines refer to the 40-, 60-, 100-, and 3,500-m water depth isobaths, respectively.

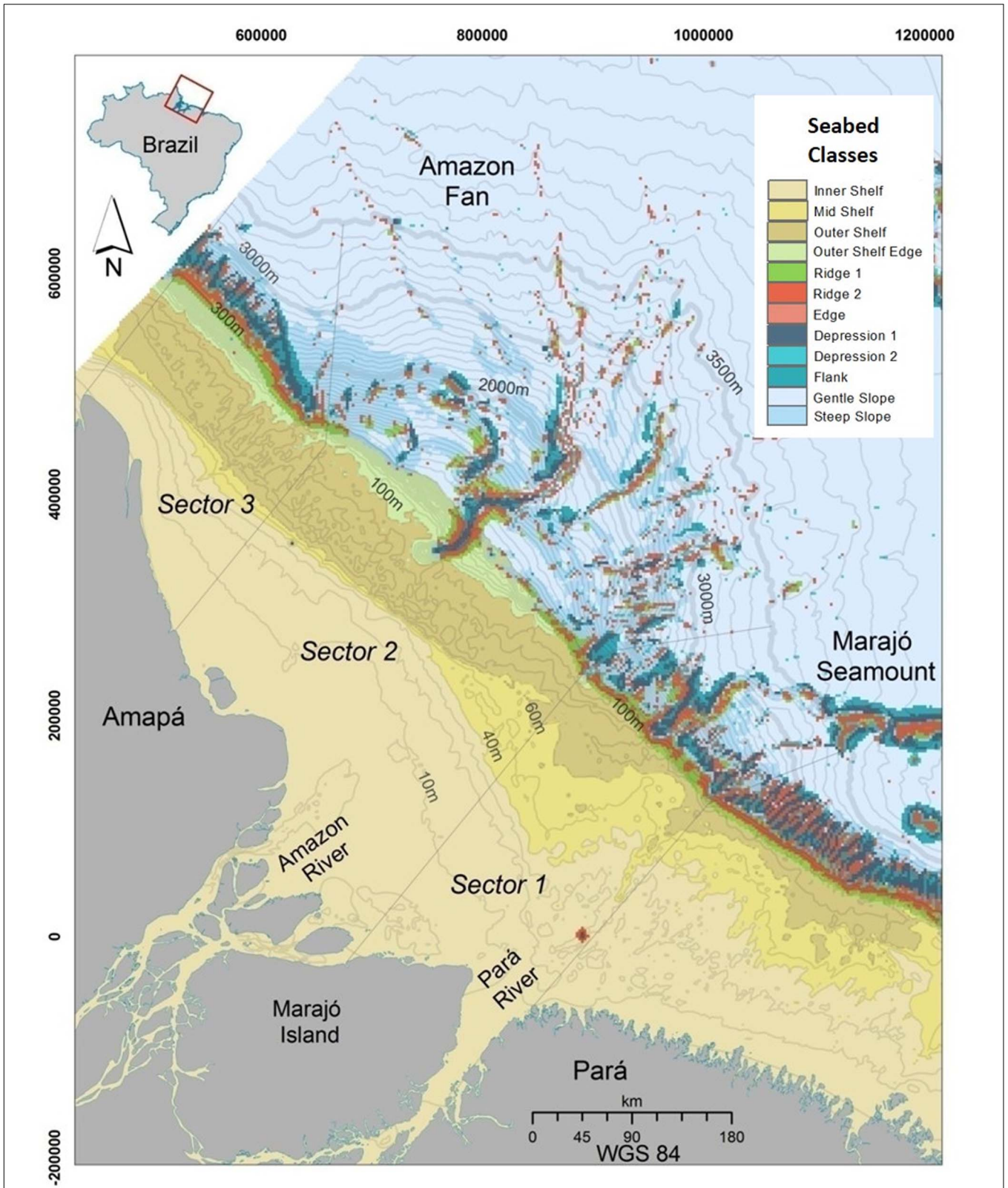

FIGURE 4 | Seabed geomorphometric classes defined with the Benthic Terrain Modeler (BTM). Isobaths are 10-m water depth spaced from the shoreline up to 300 m, and from then on, they are spaced at each 100-m interval (water depth). The thicker isobath represents 300 m, and the last one is set at 3,500 m (water depth).

respectively (**Figure 2**, top graph). Also, the transition in Sector S3 is marked by an outer shelf edge similar to a plateau or terrace, from 100- to 300-m water depth. The continental slope curvatures also differ among sectors, with Sector S1 being convex, S2 concave, and S3 sigmoidal (**Figure 2**, top graph). Slope profiles of Sectors S1 and S3 are flatter on the continental shelf portion and get steeper on the shelf edge, reaching their maximum magnitude at the shelf break zone (<6° for S1, yet >7° for S3), whereas Sector S2 is smooth across its length (<2°; **Figure 2**, bottom graph). Slope is <1° at depths higher than 3,000-m water depth in all sectors (**Figure 2**, bottom graph).

Seabed Classes

The regional bathymetry, together with the BPI models at fine and broad scales, slopes, and Aspect Analysis, results are shown in **Figure 3**, whereas the spatial distribution of the 12 seabed classes derived from the geomorphometric model is shown in **Figure 4**. Crest-related seabed classes are associated with above-mean BPI, depicting the shelf break or depression edges even in steeper regions. Depression-related seabed classes are associated with below-mean BPI, depicting elongated depressions or lower regions. The main attributes of the continental shelf and continental slope at each sector are presented in **Table 2**.

Sector 1

The continental shelf in this southernmost sector is largely flat, apart from valley edges where the slope is steeper but does not exceed 0.21° (**Figure 3C** and **Table 2**). An incise valley from 30- to 60-m depths is a remarkable feature of Sector S1 (**Figure 4**), which also presents a distinct diagonal geometry of isobaths (SE to NW oriented) that ranges from 20- to 40-m water depths. Isobaths are regular in the NW portion of the inner shelf and irregular on its SE portion (**Figure 4** and **Table 2**). Mid Shelf and Outer Shelf isobath geometry also follows the same irregular pattern (**Figure 4** and **Table 2**). Aspect (seabed dipping) on the Inner Shelf is predominantly N–NE, whereas on the Mid Shelf and Outer Shelf, there is no predominant direction (**Figure 3D**). The shelf break is located at ∼100-m water depth and is constituted by a ∼20-km-wide feature that combines seabed classes Ridge 1 and Ridge 2 (**Figure 4**). These same seabed classes form depression edges in deeper areas (**Figure 4**). The 90-km-wide continental slope is steeper (∼7.7°) from 100- to 3,500-m water depth. As depth increases, the slope becomes gentler (<0.1°), with the exception of the Marajó Seamount area (**Figure 3C** and **Table 2**). Seabed dipping orientation is mostly N–NE (**Figure 3D**).

TABLE 2 | Geomorphometric attributes of the continental shelf and continental slope at each sector.

	Sector 1	Sector 2	Sector 3
Continental shelf			
Width	330 km	390 km	230 km
Inner (∼40 m wd)	170 Regular/irregular*	200 Regular*	115 Regular*
Mid (40–60 m wd)	80 Irregular*	10–70** Regular/irregular*	4–20** Regular*
Outer (60–100 m wd)	80 Irregular*	90 Irregular*	80 Irregular*
Outer edge (100–300 m wd)	– Regular*	50 regular*	20 Regular*
Slope range	0–0.21°	0–0.47°	0–0.35°
Shelf break	100 m	No break	300 m
Continental Slope			
Width	90 km	210 km	60 km
Slope range	0.1–7.7°	6.14°	9,1°

*wd, water depth. *Isobaths configuration within the seabed class. **Mid Shelf range width, shown when the wide varies dramatically.*

Sector 2

This sector presents the widest (∼200 km) continental shelf (**Table 2**) and a relatively steep (∼0.47°) slope (**Table 2** and **Figures 3C**, **4**). The Inner Shelf presents a regular isobath geometry and shows the same diagonal pattern as S1 (from SE to NW; **Figure 4** and **Table 2**). The Mid Shelf narrows from 70 to 10 km wide, also from SE to NW (**Figure 4**). The narrower part of the Mid Shelf has a regular geometry, whereas its wider part has an irregular geometry (**Figure 4** and **Table 2**). The Outer Shelf is 90 km wide and depicts an irregular bathymetry pattern (**Figure 4** and **Table 2**). The Outer Shelf Edge (4) is 50 km wide and shows regular isobaths' geometry (**Figure 4** and **Table 2**). Seabed dipping on Sector S2 is similar to that in S1, with a regular N–NE geometry on the Inner Shelf and an irregular geometry with no prevailing direction on the Mid Shelf and Outer Shelf (**Figure 3D**). On the Outer Shelf Edge, the prevailing dipping direction is N–NE. This sector presents no sharp shelf breaking, with the Outer Shelf Edge of the continental slope comprising the 210-km-wide Amazon Fan System, between 300- and 3,500-m water depth. The Amazon Canyon incises at 100-m water depth, and its associated channels can be observed in water depths of up to 3,500 m. The slope varies considerably in this portion of the sector, being steeper on the upper (proximal) end of the fan. While Sector S2 depicts no clear shelf break, Ridge 1 and Ridge 2 seabed classes comprise depressions' edges that combine with seabed class Edges (**Figure 4**). The continental slope seabed orientation is mostly N–NE on the NE side, and N–NW on the NW side (**Figure 3D**).

Sector 3

The continental shelf of Sector S3 is manly flat, with the exception of features recorded on the Mid Shelf and valley edges on the Outer Shelf. The general slope is <0.35° (**Figure 3C** and **Table 2**). Similarly to the other sectors, the Inner Shelf and Mid Shelf seabed classes depict senoidal and parallel isobaths oriented from SE to NW (**Tables 2**, **3**), while the Outer Shelf presents an irregular isobath configuration (**Tables 2**, **3**). The Outer Shelf Edge, together with seabed classes Ridges 1 and 2, represents the shelf break zone at approximately 300-m water depth, being 35 km wide. The continental shelf seabed orientation is mainly N–NE where the isobaths configuration is regular and lacks such a regular orientation in the area with irregular isobaths (**Figure 3D**). The continental slope in Sector S3 is the steepest (9.1°) within the ACM (**Table 2**). Seabed classes

TABLE 3 | Percentage of seabed classes per sector.

	Sector 1		Sector 2		Sector 3	
(1). Inner shelf	38		33		30	
(2). Mid shelf	18		3		4	
(3). Outer shelf	10		10		25	
(4). Outer shelf edge	0.1	66.01%*	3	49%*	6	65%*
(5). Ridge 1	3		2		3	
(6). Ridge 2	4		2		3	
(7). Edges	2	9%*	2	6%*	1	7%*
(8). Depression 1	4		1		4	
(9). Flank	2		1		2	
(10). Depression 2	2	8%*	1	3%*	1	7%*
(11). Gentle slope	10		30		14	
(12). Steep slope	7	17%*	12	42%*	7	21%*

**Sum of above seabed classes.*

Depression 1, Flank and Depression 2 are present but confined to the continental slope. Edge is the only crest-associated seabed class in the continental slope of this sector. Seabed classes Steep Slope and Gentle Slope occur along the continental slope/rise. Seabed dipping orientation is mostly N–NE in the continental slope (**Figure 3**).

Shelf–Slope Transitional Features

A total of 37 depression features were mapped on the Amazon Equatorial Margin (**Figures 5–7** and **Supplementary Table S1**). Sector 1 (**Figure 5** and **Supplementary Table S1**) presented 10 such features, three of which representing shelf incised canyons, one representing a slope-confined canyon, and seven comprising slope-confined depression features. Features 1, 7, and 10 are shelf-incised canyons at 100-m water depth. Canyon 1 is the longest and most sinuous one, reaching more than 3,000-m depth range. Canyon 10 is unique in the ACM for having an associated incising valley (**Figure 4**, inc. valley). At the beginning of Canyons 6 and 7, multibeam data were used to exemplify this shelf slope transition (**Figure 5**). Despite providing different detail levels, both the BTM model and multibeam data detected both the canyon confined at the slope (Canyon 6) and the canyon incising on the continental shelf (Canyon 7).

Sector 2 (**Figure 6** and **Supplementary Table S1**) presented 15 depressions, one of which representing a shelf-incising canyon (Canyon 19). This unique feature is the so-called Amazon Canyon, with 1.840 km^2 and almost 300,000-km length and the only one that cuts the continental shelf. This sector has five slope-confined canyons nearby the Amazon Canyon, whereas the remaining nine canyons are slope confined. Sector 3 (**Figure 7** and **Supplementary Table S1**) presented 12 depressions, one of which represents a slope-confined canyon (Canyon 26). Alongside this canyon, the area mapped with multibeam covered the outer shelf and the continental slope (**Figures 8A,B**) and shows the transition from a gentle (∼0.2°) and irregular outer shelf to a steep (7°) continental slope with gullies and ravines, but lacking major canyons (**Figure 8A**). The irregular features on the Outer Shelf correspond to reef structures between 120- and 200-m water depth, herein represented in five cross-section profiles obtained from the multibeam data (profiles from 1 to 5, **Figure 9**). These structures reached 20 m in height and 450 m in length, occurring in a depth range of 120 to 200 m. Reef structures occurred either as smaller and relatively isolated patches with 10-m heights, generally concentrated in areas shallower than 130-m water depth, or as larger structures that reached 20 m in height and were concentrated in areas deeper than 130-m water depth.

Physical Megahabitats

Although other features (e.g., detailed facies and benthic community) may be considered before a comprehensive megahabitat scheme is proposed for the entire ACM, our results allow for the discrimination of at least eight of such larger compartments, three in the continental shelf, one in the shelf–slope transition, and four within the continental slope.

For the continental shelf, a Regular Mud Continental Shelf megahabitat and an Irregular Continental Shelf, which may be further divided into a Sand and a Reef compartment (**Figure 10**), were defined. The Regular Mud Continental Shelf is composed mainly by flat and irregularly oriented (SE–NW) isobaths in the Inner and Mid Shelf seabed classes, reaching no more than 60-m water depth (**Figure 10**). The Irregular Sand/Reef megahabitat is composed by the rugged parts of the Inner, Mid Shelf, and Outer Shelf seabed classes, in water depths ranging from 20 to 100 m. The slope also indicates greater roughness, and sediment distribution is dominated by sand deposits, rhodolith beds, and reefs (**Figure 10**). Sandy bottom occurs in parts of the Inner Shelf on Sector S1 (eastward of Pará River), on the Mid Shelf on Sectors S1 and S2, and on the Outer Shelf for all sectors (The Mid Shelf in Sector S2 was partially included in the Regular Mud Continental Shelf megahabitat for being part of the Amazon Delta foreset). Conversely, coarse sediments and carbonate structures are frequent on the Outer Shelf.

The shelf–slope transition megahabitat is well defined by the seabed geomorphometric classes that delineate the shelf break (Ridges 1 and 2) at Sectors S1 and S3. Also, the Outer Shelf Edge seabed class plays an important role in the definition of this megahabitat, especially in S3. Even though S2 did not depict a sharp shelf to slope transition, its smoothness could be noticed due to the presence of the Outer Shelf Edge seabed class. This megahabitat is defined by slightly increased slope values, as well as by the regular isobath geometry and N–NE prevailing seabed dipping direction.

Finally, the continental slope was subdivided in terms of the presence/absence of features such as canyons and submarine channels, resulting in four megahabitats: Featured Slope, Shallow Gentle Slope, Steep Slope, and Deep Slope. The Featured Slope megahabitat is defined by the seabed classes associated to depressions (seabed classes Depression 1, Flank, and Depression 2) and crests (Ridge 1, Ridge 2, and Edge seabed classes). The Steep Slope megahabitat occupies the areas surrounding the depressions, where the slope is still higher than 0.1°, whereas the Shallow Gentle Slope megahabitat is found in depths shallower than 2,000 m and the Deep Gentle Slope occurs below 2,000-m depth. Information about sediment facies is scarce for this latter megahabitat.

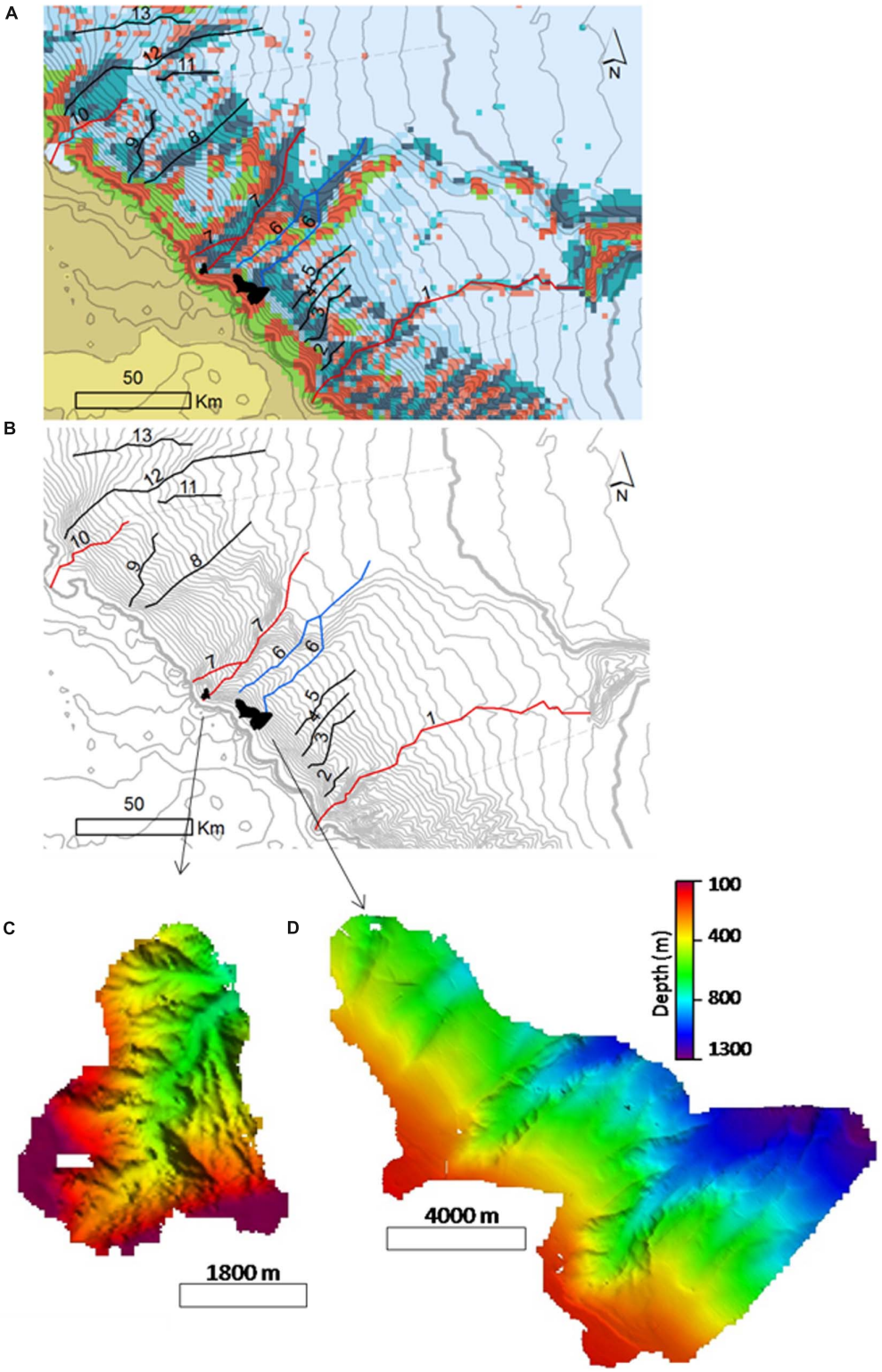

FIGURE 5 | Continental slope depressions in sector S1. Mapping procedures followed the combined methods of delineation by BTM seabed classes thalweg 1 and 2 **(A)**, and the DTM with isobaths spacing each 100-m water depth interval **(B)**. Depression types are distinguished by colors: (1) depressions not classified as canyons and confined at the continental shelf (black lines), (2) slope confined canyons (blue lines), and (3) canyons that incise the continental shelf (red lines). Arrows **(B,C)** show the location of a 40-m resolution multibeam mapped area with examples of canyons incising on the continental shelf **(C)** and canyons confined at the slope **(D)**. Vertical exaggeration 1.

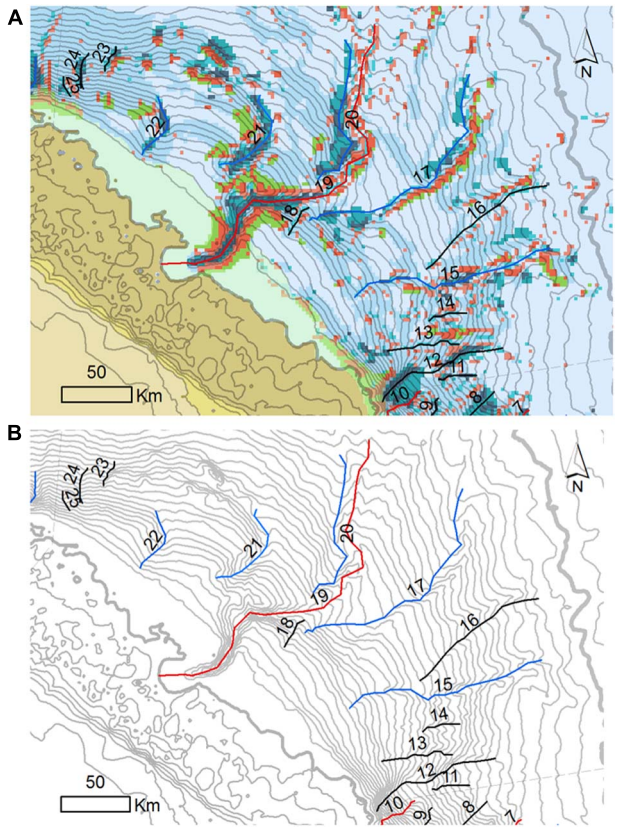

FIGURE 6 | Continental slope depressions in sector S2. Mapping procedures followed the combined methods of delineation by BTM seabed classes thalweg 1 and 2 **(A)**, and the DTM with isobaths spacing each 100-m water depth interval **(B)**. Depression types are distinguished by colors: (1) depressions not classified as canyons and confined at the continental shelf (black lines), (2) canyons that are confined to the continental slope (blue lines), and (3) canyons that incise the continental shelf (red lines).

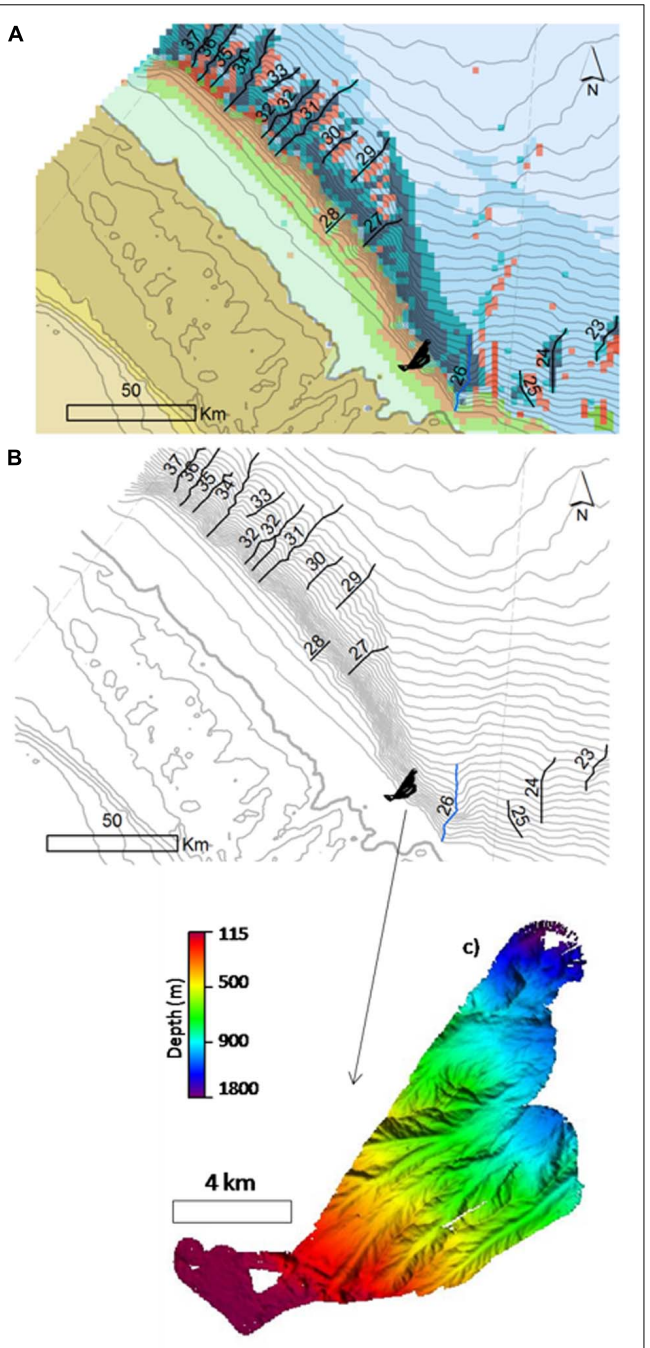

FIGURE 7 | Continental slope depressions in sector S3. Mapping procedures followed the combined methods of delineation by BTM seabed classes thalweg 1 and 2 **(A)**, and the DTM with isobaths spacing each 100-m water depth interval **(B)**. Depression types are discriminated by colors: (1) depressions not classified as canyons and confined at the continental shelf (black lines), (2) canyons that are confined to the continental slope (blue lines), and (3) canyons that incise the continental shelf (red lines). Vertical exaggeration 5.

DISCUSSION

The geomorphometric analysis of a large bathymetric dataset from the ACM allowed for a novel classification of seabed classes and a mosaic of physical benthic megahabitats, that is, large features with dimensions ranging from kilometers to tens of kilometers (Greene et al., 1999). Such seabed heterogeneity is associated to processes and environmental controls acting in different time scales, including mean sea level oscillation, gravity tectonics, and modern sedimentation. Benthic habitat classifications comprise an essential element for the analysis of ecological and fisheries data, once they help organize and describe the environment and its associated biological assemblages in a consistent manner (Costello, 2009).

Megahabitats in the ACM are strongly influenced by the modern sedimentation processes that are largely connected to semidiurnal macrotidal processes, the Amazon River outflow, persistent winds, and the NBC, which is the western boundary geostrophic current that dominates the region (Lentz, 1995; Geyer et al., 1996; Nittrouer and DeMaster, 1996).

In the Inner and Mid Shelf, megahabitats are dominated by muddy sediments (**Figure 10**) and are under a high-energy physical regime that enables unstable benthic habitats

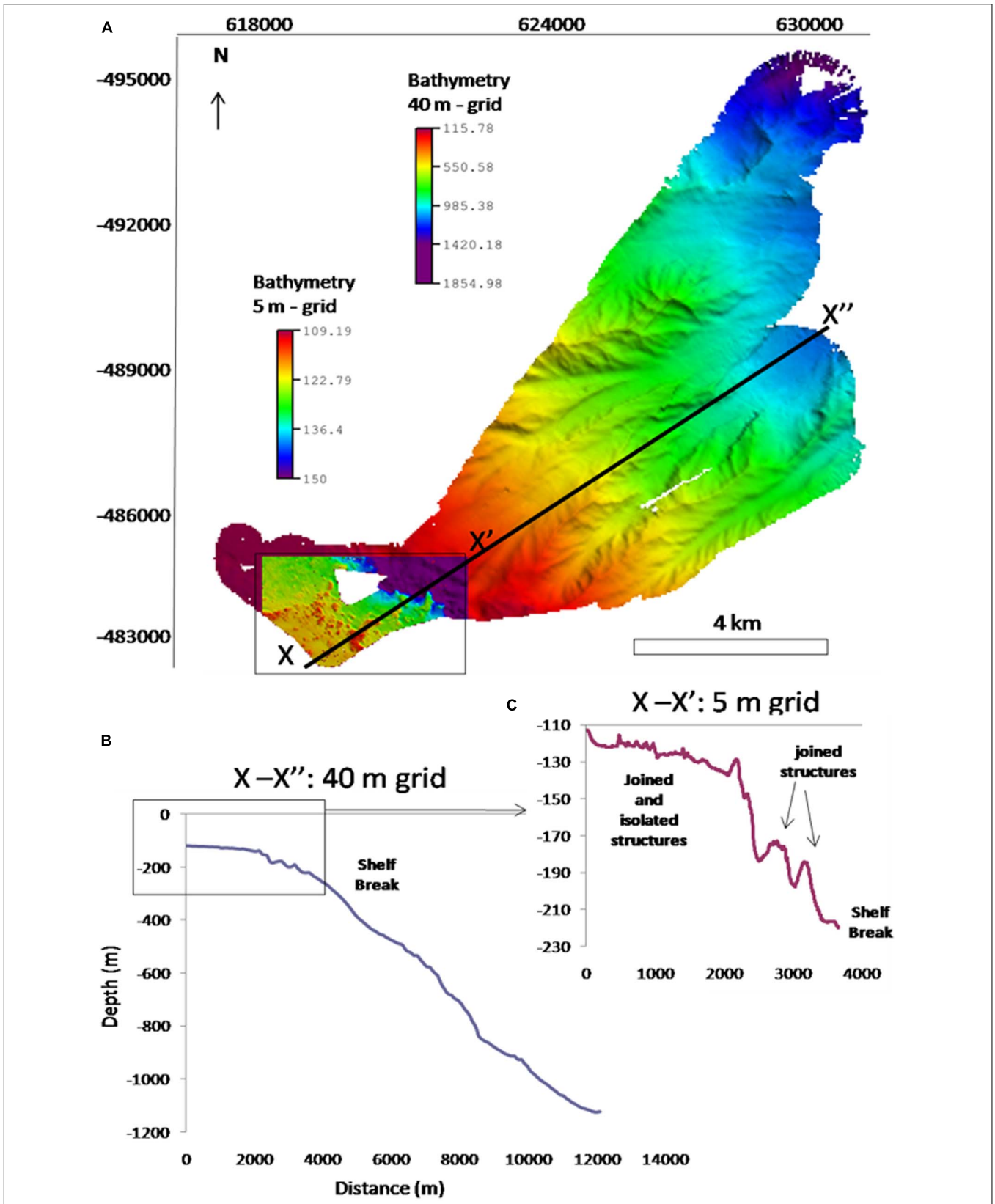

FIGURE 8 | (A) Bathymetric grids from 40- and 5-m resolution, vertical exaggeration of 3; **(B)** longitudinal profiles for the 40-m grid resolution, highlighting the black square—the 5-m grid; **(C)** longitudinal profile showing isolated and joined reefal structures and the shelf break at approximately 250- to 300-m water depth.

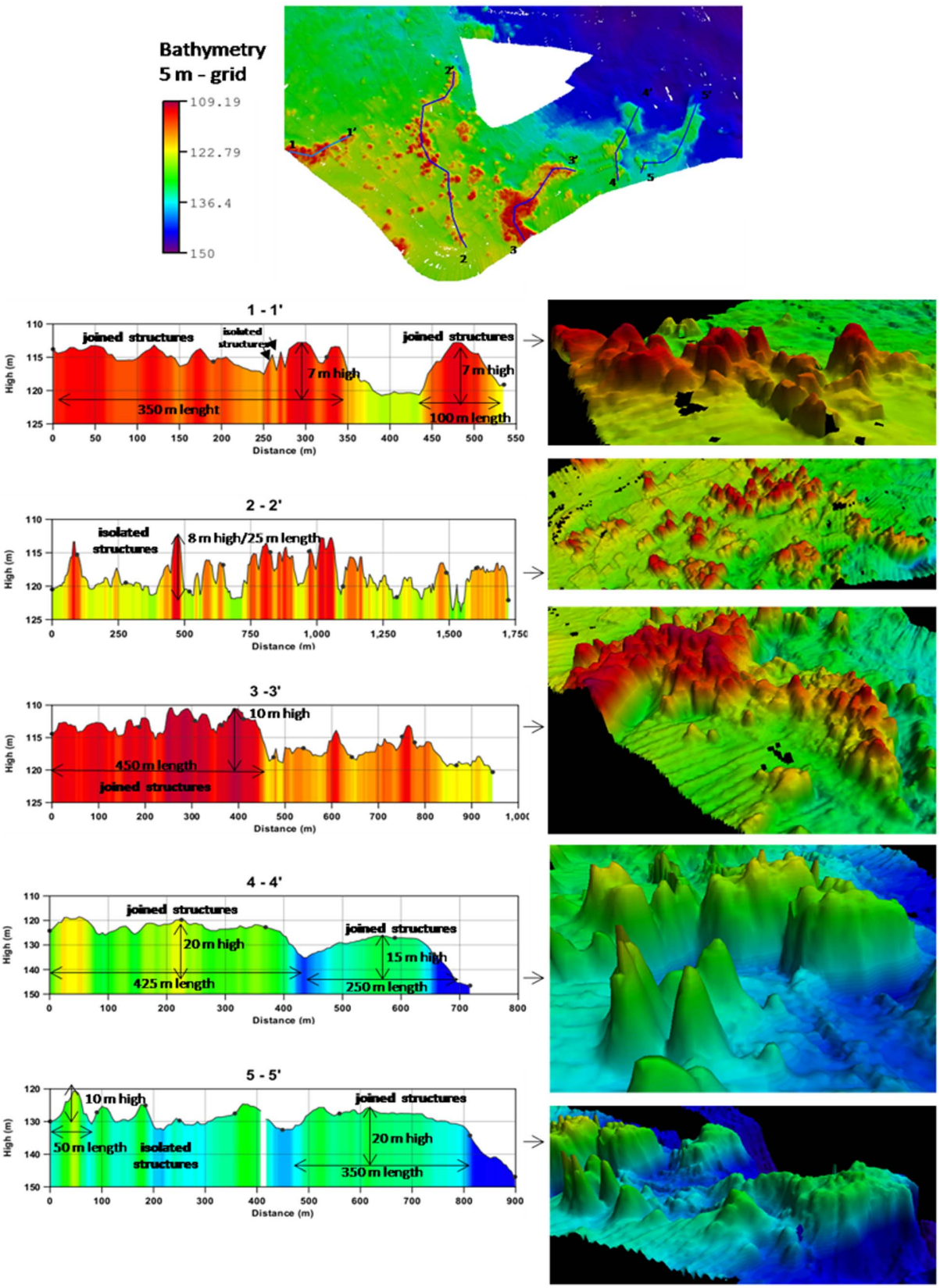

FIGURE 9 | Longitudinal profiles along the 5-m grid (from 1–5).

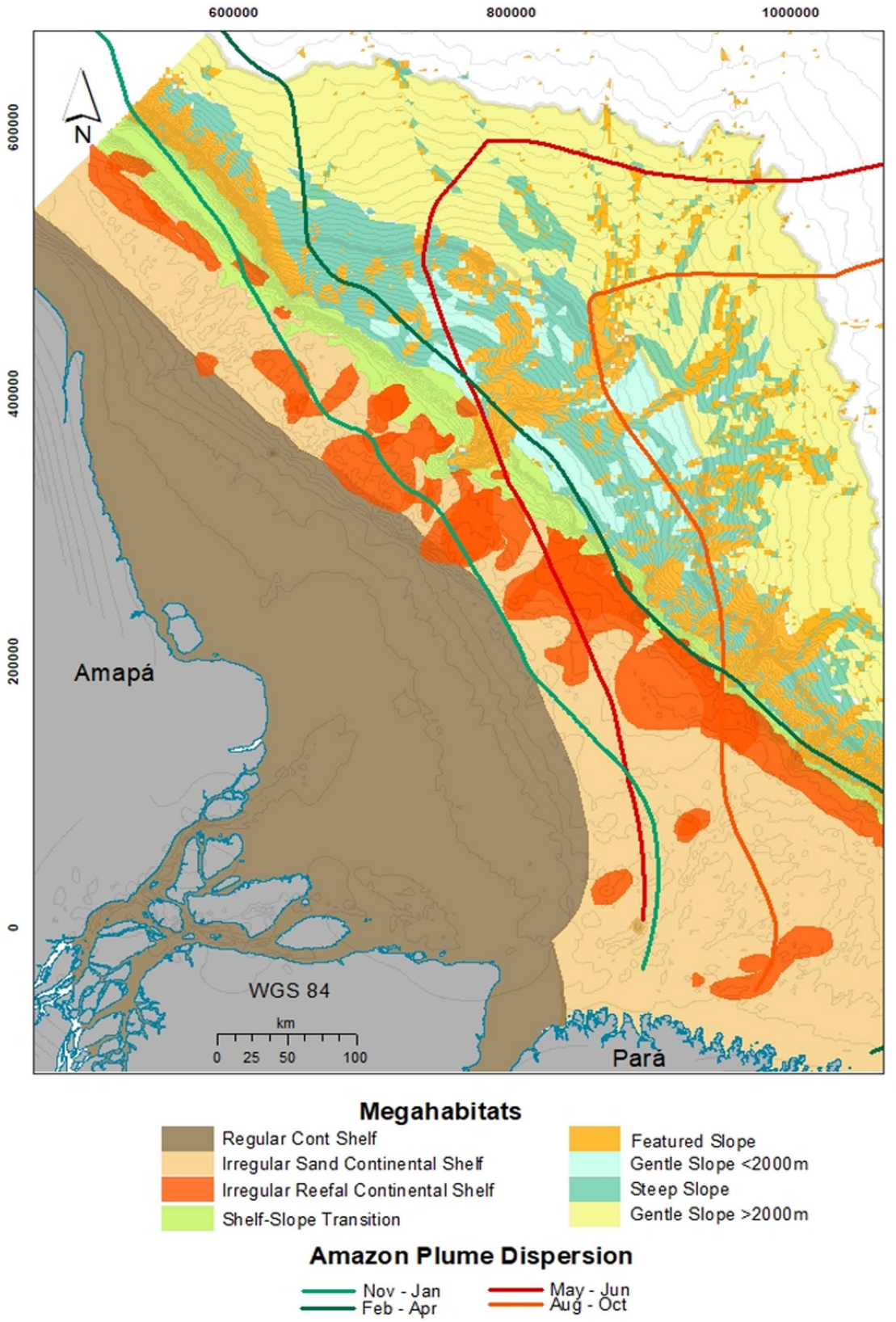

FIGURE 10 | Megahabitats of the Amazon Continental Margin as discriminated by geomorphometric analyzes.

(Nittrouer and DeMaster, 1996). Mass budgets indicate that approximately 6 × 10^6 tons per year of sediment accumulate on the inner shelf, primarily on the outer topset and foreset, at rates exceeding 10 cm/year (Kuehl et al., 1996). The diagonal NW–SE pattern of the sedimentary deposit, which presents a typical clinoform shape of a delta front, is strongly influenced by this complex physical regime (Nittrouer et al., 1996). The isobath configuration of the continental shelf, along with the N–NE prevailing seabed dipping direction, is related to the ongoing development of a clinoform that marks the subaqueous delta, as defined by Nittrouer et al. (1996). The nearly flat Inner Shelf corresponds to the landward portion of a subaqueous Amazon delta (up to 40-m water depth, topset beds), whereas the slightly steeper Mid Shelf on its NW portion, with regular geometry isobaths (S2 and S3 portions, 40- to 60-m water depths), is also part of a submerged delta foreset. The delta bottom set geomorphic feature could be identified in the Outer Shelf seabed class, from 60- to 70-m water depth on Sectors S2 and S3.

The area influenced by the Amazon Plume varies seasonally, with the Regular Continental Shelf megahabitat and part of the Irregular Shelf megahabitat constantly dominated by the Amazon Plume (**Figure 10**). Conversely, the influence of the plume over the Shelf–Slope megahabitat is more seasonal to the east of the Amazon river mouth (Moura et al., 2016). From November to April, the NW flow is associated to the combination of strong trade winds and stronger NBC transport (Geyer et al., 1996), whereas from May to October the plume retroflex eastward due to less trade winds' stress and reduced NBC transport (Geyer et al., 1996). However, 35% of the NBC flow still moves northwestward (Lentz, 1995). As a result of the NBC flow, the Amapá continental shelf (Sector S3) is the greatest sediment depocenter.

The Irregular Sand/Reef megahabitats are under lower influence of sediment input fluvial discharge dominance, together with the strong currents, making this habitat a suitable environment for carbonate occurrence. **Figure 11** shows images of these megahabitats. The outer shelf in Sector S1 is under less influence of the plume, and it is where younger carbonates were observed in comparison to S3, which is under permanent riverine influence (Moura et al., 2016; Vale et al., 2018). The occurrence of carbonate structures in a prevailing turbid environment can be explained by the role played by the NBC (Geyer et al., 1996; Nittrouer and DeMaster, 1996), preventing terrigenous sedimentation from burying reef structures and resulting in the complex hard bottom topography (Moura et al., 2016). Such a low sediment accumulation zone can also be related with a permanent frontal pressure gradient, as well as to Ekman transport associated with the advection of relatively cold and non-turbid waters across the outer and mid shelf (Geyer et al., 1996; Nittrouer and DeMaster, 1996).

The paleovalley observed in Sector S1 is probably associated to Canyon 1 (**Figures 4**, **5A,B**). These features were possibly connected in the last glacial period, when sea level was about 120 m lower than in the present (Milliman et al., 1975). However, the paleovalley associated with the Amazon Canyon (**Figures 4**, **5A,B**; Canyon 19), in Sector S2, is not recognized within our continental shelf dataset. One possible reason for this is related to carbonates' prevalence on S1, which led to the major preservation of paleovalleys. Also, the high sedimentation that subdued this portion of the continental shelf when sea level started to rise (Sommerfield et al., 1995) probably, led to the burial of the channel. In general, the stratigraphic record created on the Amazon shelf is punctuated by hiatuses caused by high-energy conditions and erosional processes occurring at different time scales (Sommerfield et al., 1995; Nittrouer et al., 1996).

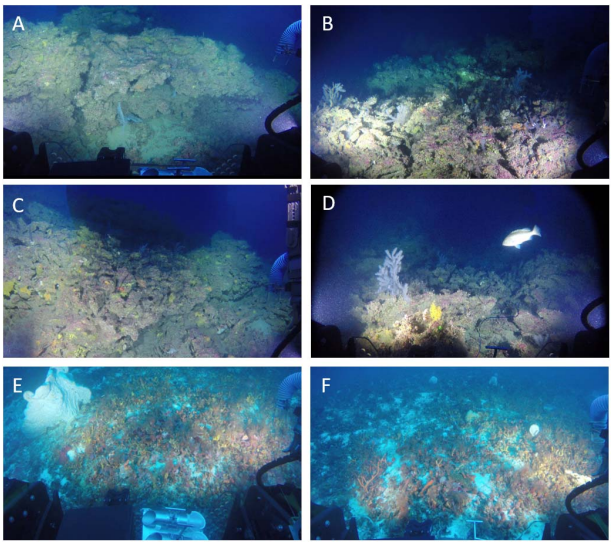

FIGURE 11 | Underwater images **(A–D)** are images from the shelf-edge reef in S3; images **(E,F)** show the rhodolith beds and associated mesophotic community along the mid-outer shelf classes in S1. Photographs taken from a submersible.

The shelf break in the shelf–slope transition varies significantly among sectors, from approximately 100-m water depth at Sector S1 (concave curvature) to 300-m water depth at S3 (sigmoidal), whereas in S2 (convex) there is no defined shelf break. The continental shelf enlargement from Sectors S1 to S3 can be explained by the predominant direction of the Amazon River sediment load. The high load of sediment on Sector S3, since the establishment of the Amazon basin drainage 2.5 Ma BP (Figueiredo et al., 2009; Gorini et al., 2014; Cruz et al., 2019), is associated to its deeper continental shelf (reaching 300-m water depth), whereas the lack of sediment arriving on S1 is associated to a shallower shelf break at approximately 100-m water depth. The shelf–slope transition megahabitat is also dominated by carbonate sedimentation and structures, which are more developed on Sector S1 (Outer Shelf and Shelf-Slope classes) probably due to the lower fluvial dominance. The area mapped with multibeam in Sector S3 showed submerged or drowned structures (**Figures 11A–D**) that possibly constitute an important geological record of sea-level variations and deserve further investigations. Reef building at the edges of continental shelves was common throughout the world during the LGM low stand sea level, with examples in the South Pacific (Flamand et al., 2008), Hawaii (Webster et al., 2004), Caribbean (Blanchon et al., 2002), and Australia (Woodroffe et al., 2010;

Abbey et al., 2011), among others (review in Montaggioni, 2000), and now it is reported in the Equatorial Atlantic margin. The rapid deglaciation process led to high rates of accommodation-space creation, and most of these shelf-edge reefs could not keep up with sea level rise, leaving behind a give-up reef (Neumann and Macintyre, 1985). These reefs are currently distributed from ∼30- to 200-m water depths and are colonized by modern mesophotic benthic assemblages (Hinderstein et al., 2010; Abbey et al., 2011). These reef zones provide structural habitats for a variety of organisms (Hinderstein et al., 2010) and thus are considered by many authors as extensions of shallow reefs and may have biological, physical, and chemical connectivity with the latter, thus having associated communities (Hinderstein et al., 2010; Harris and Whiteway, 2011). In the Great Barrier Reef (GBR), Bridge et al. (2012) showed a depth gradient change in the dominated mesophotic community from photosynthetic organisms in shallower reefs (40 m) to filter feeders dominated in deeper reefs (100 m deep).

In Australia's GBR, Abbey et al. (2013) showed that two generations of mesophotic communities have developed on shelf-edge reefs, one between 13,000 and 10,000 years BP and another from 8,000 years BP to the present. Thus, the reef structures mapped herein at approximately 120 m deep can be interpreted as relict shelf-edge reefs with an associated mesophotic community, as reported by Moura et al. (2016). Although based on a single petrographic analysis from the ACM (Sector S3), Moura et al. (2016) indicated a microfacies of an older grainstone (12,100 ± 30,000 years BP) and composed by filter feeders (polychaetes, foraminifera, barnacles, bryozoans, and mollusks) under a thin veener of coralline algae, which seems to correspond to the situation described by Abbey et al. (2013) for the GBR. The age of the surface of a reef structure at the shelf edge in Sector S3 is 13,382 to 12,749 calibrated years BP (Moura et al., 2016), corresponding to the late stages of the last postglacial maximum transgression. In Sector S1, rhodoliths and calcareous algae reefs are younger, dated from 4,487 calibrated years BP to modern ages (Moura et al., 2016; Vale et al., 2018). This longshore trend shows the shutdown gradient of the reefs, from marginal reef growth and recent shutdown in Sector S1 to a persistent turn off state during thousands of years in Sector S3. Reef growth off the Amazon mouth during the LGM seems to be associated to the bypass of sediments to the deep sea, through an active Amazon Submarine Canyon, and also to the turning off of the muddy channels in the shelf (Gorini et al., 2014; Cruz et al., 2019), enabling shallow water biogenic and oolitic carbonates accumulation off the Amazon River. Considering that there are living mesophotic communities (**Figure 11**), the growth of reef structures is active along part of the ACM but, possibly, with very small growth rates. The reefs, including the rhodolith beds, support highly diverse associated mesophotic communities and relevant ecosystem services (Collette and Rutzler, 1977; Cordeiro et al., 2015; Moura et al., 2016). Indeed, most reef fisheries in the ACM (lobsters and snappers) are carried out in and near these structures (Moura et al., 2016).

In terms of slope-transition habitats, the types of depressions (morphometric features) vary markedly among sectors. Sectors S1 and S3 are erosive, whereas sector S2 is non-erosive. Gravity tectonics was the main driver responsible for shaping the erosive and non-erosive continental slope over the time (Reis et al., 2016). The great amount of sediments that reached the shelf–slope transition through the geological time generates mass movements that lead to steep scarps and mega slides (Silva et al., 2010; Reis et al., 2016). Sediment input is related to the heterogeneous continental slope morphometry among sectors. The slope transition curvature is convex in S2, where most sediment input occurs and where the Amazon Cone was formed. In the erosive part of the region, depressions in S1 begin in shallower waters, approximately 100-m water depth. This is the sector that depicts more canyons incising the continental shelf (Canyons 1, 7, and 10). For instance, depressions in S1 are longer and more sinuous and present lower slope value depressions than those in S3, which begin in deeper water and follow the occurrence of a distinct shelf-edge area in which the shelf breaks at approximately 300-m depth. Depressions in S3 are shorter and less sinuous and present higher slope values than those in S1. In the non-erosive part of the continental slope (Sector S2), the Amazon Canyon is always active during low stand, when the immense amount of sediments caused a turbidity current that was responsible for developing the great canyon (Figueiredo et al., 2009; Gorini et al., 2014). The Amazon Canyon (Canyon 19) is the only depression in S2 that incises the shelf, but five slope-confined canyons are recorded in this sector. Depressions are the most sinuous and present lower slope values. On the NW portion of the Fan, there are fewer and shorter canyons, whereas on the SE portion, canyons are longer. The abrupt distinction of NW and SE portion are associated to N–NW and N–NE seabed dipping orientation, respectively.

The Slope megahabitats comprise a great number of morphometric classes and morphological features associated with canyons and channels, as evidenced in **Figures 4–7**. This makes the ACM Slope classes a potential high-diversity deep-sea habitat, especially when combined with the shelf–slope transition megahabitat. The Features Slope megahabitat (with depressions/canyons) should be prioritized in future assessments targeted at the geobiodiversity of the ACM. The areas where no depressions are observed were classified as the Depression Free Megahabitat. This megahabitat is well defined by the Gentle Slope seabed geomorphometric class. This habitat is in >2,000-m water depth, representing the base of the slope/continental rise and the beginning of the abyssal plain. The deeper areas seem to correspond to the start of sediment accumulation in deep basin (Harris et al., 2014), with gentle slope values and a general lack of other features.

Akin to the continental shelf, which presents a great diversity of facies (Dutra, 2018), the Continental Slope Megahabitat could also be further classified in mesohabitats and macrohabitats if other investigation scales are considered. Considering the important role played by the gravitational tectonics in shaping the seafloor, seafloor higher-resolution data have shown that gravitational collapse is expressed at seabed as ridges formed by paired extensional–compressional belts and thrust faults (Reis et al., 2016; Ketzer et al., 2018). In some areas of the upper slope, gas seeps are observed in association with these faults, which could be another important driver for supporting specific

deep-sea habitats. **Figure 4** depicts a few Steeper Slope Classes in a more distal part of the Amazon Fan. It is possible that changes in slope angle, creating a rough topography, are related to seabed deformation due to the mega mass transport deposits (Reis et al., 2016).

The geomorphometric analysis presented herein revealed novel dimensions of the spatial structuring of megahabitats along cross-shelf and longshore gradients of the ACM. Such marked spatial structuring is largely associated to the interaction of short-mid and long-term geological and oceanographic processes operating in the broad continental shelf and slope off the mouth of the world's largest river. The stronger morphometric heterogeneity found along the Outer Shelf and Outer Shelf Edge megahabitats was also very distinct among the three sectors. Sector S3 is remarkable for presenting the outer shelf edge and ridges together and for encompassing the significant erosive reef structures identified by Moura et al. (2016), which were described herein in greater detail (see **Figures 7–9**, **11**). In a sharp contrast, Sector S2 presents no shelf break and is associated with the long-term sediment accumulation of the Amazon Fan, whereas S1 shows a number of valley incised channels in the shelf, representing an erosive area with main sediment bypass and carbonate sedimentation, especially due to the presence of extensive rhodolith beds. The occurrence of depressions (canyons, ravines, or gullies), especially in Sector S1, adds to the geomorphologic heterogeneity of the shelf–slope transition and the Continental Slope megahabitat, which encompass several macrohabitats.

Besides providing an initial overview of the benthic mosaic of megahabitats in the ACM, our results highlight a number of potential targets for future geodiversity and biodiversity assessments, which are greatly needed for the implementation of a marine spatial planning initiative in this globally relevant region that is under growing pressures from several sectors (oil and gas, fisheries).

CONCLUSION

A digital terrain model allowed us to discriminate eight megahabitats in the ACM: Regular Mud, Irregular Sand, and Carbonate Continental Shelf, Shelf–Slope Transition, Featured Slope, Shallow Gentle Slope (<2,000 m), and Steep Slope, Deep Gentle Slope (>2,000 m). The distribution of these megahabitats is related to distinct geological and oceanographic processes that operate over different time scales.

Megahabitats in the continental shelf are basically controlled by the Amazon River discharge and sediment input, especially the Regular Mud Continental Shelf megahabitat, which comprises the main depocenter in Sector S3. The Irregular Sand/Carbonate Continental Shelf megahabitat is seasonally influenced by the Amazon plume and, along the outer shelf, is influenced by the strong flow of the NBC, which enables carbonate production, the formation of large sand waves, and the persistence of unburied reef structures.

The shelf–slope transition megahabitat varies significantly along the shelf break due to long-term sediment accumulation, river incisions, and gravitational tectonics. The shelf break depth varies among all the sectors from approximately 100-m water depth at Sector S1 down to 300-m water depth at S3, where the outer shelf edge is well defined and the shelf lacks incised valleys. Sector S2 represents the transition to the Amazon fan, which is the most important long-term sediment pathway to the slope and rise.

The Featured Slope megahabitat is formed by channel incisions (canyons, ravines, or gullies) and megaslides. Akin to the shelf–slope transition megahabitat, Sector S2 is very distinct, as it comprises the Amazon Fan and the Amazon deep channel. This is the most diverse habitat and comprises the greatest number of seabed classes defined by the terrain analysis. Megahabitats Shallow Gentle Slope (<2,000 m), Steep Slope, and Deep Gentle Slope (>2,000 m) are less morphologically diverse.

The ACM represents one of the world's most complex and dynamic continental margins, due to its long-term interaction with the Amazon River. In addition, the ACM is under increasing pressure from several sectors (e.g., oil and gas, mining), but comprehensive habitat mapping is still largely incomplete. Our results confirm that geomorphometric analyses comprise a relevant tool to define benthic megahabitats and may be used for triggering a much-needed spatial planning process in the ACM.

DATA AVAILABILITY STATEMENT

The regional bathymetric dataset can be found in the https://www.marinha.mil.br/dhn/q=node/249. The multibeam data is available on request to the corresponding author.

AUTHOR CONTRIBUTIONS

AB, RM, and FM designed the survey and collected the multibeam data. All authors contributed to the writing and review of the manuscript. AL and AB designed the investigation with the BTM. AL conducted the multibeam processing and BTM modeling.

FUNDING

AL had a post-graduate scholarship from CAPES (Ministry of Education, Brazil) to develop this research. Financial support to the acoustic survey and the follow up of AL research was provided by an ANP/Brasoil grant. AB and RM acknowledge CNPq (Ministry of Science, Technology, Innovation and Communications, Brazil) and CAPES/IODP grants. Paulo S. Salomon, Fabio S. Motta, Leonardo M. Neves, and Milton Kampel also provided invaluable field support.

ACKNOWLEDGMENTS

We thank the Brazilian Navy Hydrographic Office for providing the compiled bathymetric dataset. We are also very much thankful to Dalio Philanthropies and OceanX, Woods

Hole Oceanographic Institution and the M/V Alucia Vessel crew for supporting the project and for providing technical assistance with data collection. We dedicate this contribution to the memory of our dear team leader, GA, who passed away in March 2019.

SUPPLEMENTARY MATERIAL

The Supplementary Material for this article can be found online at: https://www.frontiersin.org/articles/10.3389/fmars.2020.00190/full#supplementary-material

REFERENCES

Abbey, E., Webster, J. M., and Beaman, R. (2011). Geomorphology of submerged reefs on the shelf edge of the Great Barrier Reef: the influence of oscillating Pleistocene sea-levels. *Mar Geol.* 288, 61–78. doi: 10.1016/j.margeo.2011.08.006

Abbey, E., Webster, J. M., Braga, J. C., Thorogood, G., Thomas, A. L., Camoin, P. J., et al. (2013). Deglacial mesophotic reef demise on the Great Barrier Reef. *Palaeogeogr. Palaeoclimatol. Palaeoecol.* 392, 473–494. doi: 10.1016/j.palaeo.2013.09.032

Barreto, L. A., Milliman, J. D., Amaral, C. A., and Francisconi, O. (1975). Upper continental margin sedimentation off Brazil, northern Brazil. *Contr. Sedimentol.* 4, 11–43.

Blanchon, P., Jones, B., and Ford, D. C. (2002). Discovery of a submerged relic reef and shoreline off Grand Cayman: further support for an early Holocene jump in sea level. *Sediment Geol.* 147, 253–270. doi: 10.1016/S0037-0738(01)00143-149

Brandão, J. A., and Feijó, F. J. (1994). Bacia foz do amazonas. *Bol. Geoc. Petrobras.* 8, 91–99.

Bridge, T., Beaman, R., Done, T., and Webster, J. (2012). Predicting the location and spatial extent of submerged coral reef habitat in the great barrier reef world heritage area. Australia. *PLoS One* 7:e0048203. doi: 10.1371/journal.pone.0048203

Campbell, A. E. (2005). Shelf-geometry response to changes in relative sea level on a mixed carbonate-siliciclastic shelf in the Guyana Basin. *Sediment. Geol.* 175, 259–275. doi: 10.1016/j.sedgeo.2004.09.003

Coles, V. J., Brooks, M. T., Hopkins, J., Stukel, M., Yager, P., and Hood, R. R. (2013). The pathways and properties of the Amazon river plume in the tropical North Atlantic Ocean. *J. Geophys. Res. Ocean.* 118, 6894–6913. doi: 10.1002/2013JC008981

Collette, B. B., and Rutzler, K. (1977). "Reef fishes over sponge bottoms of the mouth of Amazon River," in *Proceedings of the Third International Coral Reef Symposium*, Miami, FL, 305–310.

Cordeiro, R. T. S., Neves, B. M., Rosa-Filho, J. S., and Pérez, C. D. (2015). Mesophotic coral ecosystems occur offshore and north of the Amazon River. *Bull. Mar. Sci.* 91, 491–510. doi: 10.5343/bms.2015.1025

Costello, M. J. (2009). Distinguishing marine habitat classification concepts forecological data management. *Mar. Ecol. Prog. Ser.* 397, 253–268. doi: 10.3354/meps08317

Cruz, A. M., Reis, A. T., Suc, J. P., Silva, C. G., Praeg, D., Granjeon, D., et al. (2019). Neogene evolution and demise of the Amapá carbonate platform, Amazon continental margin, Brazil. *Mar. Petrol. Geol.* 105, 185–203. doi: 10.1016/j.marpetgeo.2019.04.009

Damuth, J. E., and Fairbridge, R. W. (1970). Equatorial atlantic deep-sea arkosic sands and ice-age aridity in tropical South America. *Geol. Soc. Am. Bull.* 81, 2181–2202. doi: 10.1130/0016-7606197081

Damuth, J. E., and Flood, R. D. (1984). Morphology, sedimentation processes, and growth pattern of the Amazon Deep-Sea Fan. *Geo Mar. Lett.* 3, 109–117. doi: 10.1007/BF02462455

Damuth, J. E., Flood, R. D., Kowsmann, R. O., Belderson, R. H., and Gorini, M. A. (1988). Anatomy and growth pattern of amazon deep-sea fan as revealed by long-range side-scan sonar (GLORIA) and high-resolution seismic studies. *AAPG Bull.* 72:30.

Damuth, J. E., and Kumar, N. (1975). Amazon cone: morphology, sediments, and growth pattern. *Geol. Soc. Am. Bull.* 86, 863–878.

Dutra, L. (2018). *Growing Industrialization Challenges Biodiversity Conservation And Natural Resources Management In The Amazon Shelf Off Brazil*. Dissertação de Mestrado, Universidade Federal do Rio de Janeiro, Brasil.

Erdey-Heydorn, M. (2008). An ArcGIS seabed characterization toolbox developed for investigating benthic habitats. *Mar. Geod.* 31, 318–358. doi: 10.1080/01490410802466819

Figueiredo, J., Hoorn, C., Van der Ven, P., and Soares, E. (2009). Late miocene onset of the amazon river and the amazon deep-sea fan: evidence from the foz do amazonas Basin. *Geology* 37, 619–622. doi: 10.1130/G25567A.1

Figueiredo, J., Zálan, P. V., and Soares, E. F. (2007). Bacia da Foz do Amazonas. *Bol. Geociências Petrob.* 15, 299–309.

Flamand, B., Cabioch, G., Payri, C., and Pelletier, B. (2008). Nature and biological composition of the New Caledonian outer barrier reef slopes. *Mar. Geol.* 250, 157–179. doi: 10.1016/j.margeo.2007.12.002

Francini-Filho, R., Asp, N., Siegle, E., Hocevar, J., Lowyck, K., D'Avila, N., et al. (2018). Perspectives on the great amazon reef: extension. biodiversity and threats. *Front. Mar. Sci.* 5:142. doi: 10.3389/fmars.2018.00142

Geyer, W., Beardsley, R. C., Lentz, S. J., Candela, J., Limeburner, R., Johns, W. E., et al. (1996). Physical oceanography of the Amazon shelf. *Cont. Shelf Res.* 16, 575–616. doi: 10.1016/0278-4343(95)00051-8

Gorini, C., Haq, B. U., dos Reis, A. T., Silva, C. G., Cruz, A. M., Soares, E., et al. (2014). Late neogene sequence stratigraphic evolution of the foz do amazonas basin. Brazil. *Terra Nov.* 26, 179–185. doi: 10.1111/ter.12083

Greene, G., Yoklavich, M., Starr, R., O'Connell, V., Wakefield, W., Sullivan, D., et al. (1999). A classification scheme for deep seafloor habitats. *Oceanol. Acya* 22, 663–678. doi: 10.1016/s0399-1784(00)88957-4

Harris, P. T., Macmillan-Lawler, M., Rupp, J., and Baker, E. K. (2014). Geomorphology of the oceans. *Mar. Geol.* 352, 4–24. doi: 10.1016/j.margeo.2014.01.011

Harris, P. T., and Whiteway, T. (2011). Global distribution of large submarine canyons: geomorphic differences between active and passive continental margins. *Mar Geol.* 285, 69–86. doi: 10.1016/j.margeo.2011.05.008

Hinderstein, L. M., Marr, J. C. A., Martinez, F. A., Dowgiallo, M. J., Puglise, K., Pyle, R. L., et al. (2010). Theme section on "mesophotic coral ecosystems: characterization, ecology, and management." *Coral. Reefs* 29, 247–251. doi: 10.1007/s00338-010-0614-5

Hoorn, C., Guerrero, J., Sarmiento, G., and Lorente, M. (1995). Andean tectonics as a cause forchanging drainage patterns in Miocene northern South America. *Geology* 23, 237–240.

Ketzer, J. M., Augustin, A., Rodrigues, L. F., Oliveira, R., Praeg, D., Pivel, M. A. G., et al. (2018). Gas seeps and gas hydrates in the Amazon deep-sea fan. *Geo Mar. Lett.* 38, 429–438. doi: 10.1007/s00367-018-0546-6

Kuehl, S. A., Nittrouer, C. A., Allison, M. A., Faria, L. E. C., Dakut, D. A., Maeger, J. M., et al. (1996). Sediment deposition, accumulation, and seabed dynamics in an energetic fine-grained coastal environment. *Cont. Shelf Res.* 16, 787–815. doi: 10.1016/0278-4343(95)00047-x

Kuehl, S. A., Nittrouer, C. A., and DeMaster, D. J. (1986). Distribution of sedimentary structures in the Amazon subaqueous delta. *Cont. Shelf Res.* 6, 311–336. doi: 10.1016/0278-4343(86)90066-X

Kumar, N., Damuth, J. E., and Gorini, M. A. (1977). Discussion: relict magnesian calcite oolite and subsidence of the Amazon shelf. *Sedimentology* 24, 143–148. doi: 10.1111/j.1365-3091.1977.tb00124.x

Lecours, V., Dolan, M. F. J., Micallef, A., and Lucieer, V. L. (2016). A review of marine geomorphometry, the quantitative study of the seafloor. *Hydrol. Earth Syst. Sci.* 20, 3207–3244. doi: 10.5194/hess-20-3207-2016

Lentz, S. J. (1995). Amazon Plume inferred from historical hydrographic. *J. Geophys. Res.* 100, 2391–2400.

Lundblad, E., Wright, D., and Miller, J. (2006). Classifying benthic terrains with multibeam bathymetry, bathymetric position and rugosity: Tutuila, American Samoa. *Mar. Geodesy.* 29, 89–111.

Meade, R., Rodrigues, F., Carlos, V., and John, E. (1979). Sediment loads in the Amazon River. *Nature* 278:3. doi: 10.1016/j.zool.2016.07.003

Milani, E. J., Brandão, J. A., Zálan, P. V., and Gamboa, L. A. P. (2001). Petróleo na margem continental brasileira: geologia, exploração, resultados e perspectivas. *Braz. J. Geophys.* 18, 351–396.

Milliman, J. D., and Barretto, H. T. (1975a). Relict magnesian calcite oolite and subsidence of the Amazon shelf. *Sedimentology* 22, 137–145. doi: 10.1111/j.1365-3091.1975.tb00288.x

Milliman, J. D., and Barretto, H. T. (1975b). Upper continental margin sedimentation off Brazil. *Contribut. Sedimentol.* 4, 1–10.

Milliman, J. D., Butenko, J., Barbot, J. P., and Hedberg, J. (1982). Depositional patterns of modern Orinoco/Amazon muds on the northern Venezuelan shelf. *J. .Mar. Res.* 40, 643–657.

Milliman, J. D., Summerhayes, C. P., and Barretto, H. T. (1975). Quaternary sedimentation on the amazon continental margin: a model. *Bull. Geol. Soc. Am.* 86, 610–614.

Montaggioni, L. (2000). Post glacial reef growth. *Earth Planet Sci. Lett.* 331, 319–330.

Moura, R. L., Amado-filho, G. M., Moraes, F. C., Brassileiro, P. S., Salomon, P. S., Mahiques, M. M., et al. (2016). An extensive reef system at the Amazon River mouth. *Sci. Adv.* 2, 1–12. doi: 10.1126/sciadv.1501252

Moura, R. L., Secchin, N. A., Amado-Filho, G. M., Francini-Filho, R. B., Freitas, M. O., Minte-Vera, C. V., et al. (2013). Spatial patterns of benthic megahabitats and conservation planning in the Abrolhos Bank. *Continental. Shelf Res.* 70, 109–117. doi: 10.1016/j.csr.2013.04.036

Neumann, A. C., and Macintyre, I. (1985). "Reef response to sea level rise: keep-up, catch-up or give up," in *Proceedings of the 5th International Coral Reef Congress*, Tahiti, 105–110.

Nittrouer, C. A., and DeMaster, D. J. (1986). Sedimentary processes on the Amazon continental shelf: past, present and future research. *Cont. Shelf. Res.* 6, 5–30. doi: 10.1016/0278-4343(86)90051-8

Nittrouer, C. A., and DeMaster, D. J. (1996). The Amazon shelf setting: tropical, energetic, and influenced by a large river. *Cont. Shelf. Res.* 16, 553–573. doi: 10.1016/0278-4343(95)00069-0

Nittrouer, C. A., Kuehl, S. A., DeMaster, D. J., and Kowsmann, R. O. (1986). The deltaic nature of Amazon shelf sedimentation. *Geol. Soc. Am. Bull.* 97, 444–458.

Nittrouer, C. A., Kuehl, S. A., Figueiredo, A. G., Allison, M. A., Sommerfield, C. K., Rine, J. M., et al. (1996). The geological record preserved by Amazon shelf sedimentation. *Cont. Shelf. Res.* 16, 817–841. doi: 10.1016/0278-4343(95)00053-4

Reis, A. T., Araújo, E., Silva, C. G., Cruz, A., Gorini, C., Droz, L., et al. (2016). Effects of a regional décollement level for gravity tectonics on late Neogene to recent large-scale slope instabilities in the Foz do Amazonas Basin. *Brazil. Mar. Pet. Geol.* 75, 29–52. doi: 10.1016/j.marpetgeo.2016.04.011

Reis, A. T., Perovano, R., Silva, C. G., Vendeville, B. C., Araujo, E., Gorini, C., et al. (2010). Two-scale gravitational collapse in the Amazon Fan: a coupled system of gravity tectonics and mass-transport processes. *J. Geol. Soc. Lond.* 167, 593–604. doi: 10.1144/0016-76492009-035

Silva, C. G., Araújo, E., and Reis, A. T. (2010). "Advances in natural and technological hazards research", in *Submarine Mass Movements and Their Consequences*, eds J. Locat, J. Mienert, and L. Boisvert (Dordrecht: Springer Science), 1–540. doi: 10.1007/978-94-010-0093-2

Silva, S. R. P., Maciel, R. R., and Severino, M. C. G. (1999). Cenozoic tectonics of Amazon Mouth Basin. *Geo Mar. Lett.* 18, 256–262. doi: 10.1007/s003670050077

Sommerfield, C. K., Nittrouer, C. A., and Figueiredo, A. G. (1995). Stratigraphic evidence of changes in Amazon shelf sedimentation during the late Holocene. *Mar. Geol.* 125, 351–371. doi: 10.1016/0025-3227(95)00019-U

Vale, N. F., Amado-Filho, G. M., Braga, J. C., Brasileiro, P. S., Karez, C. S., Moraes, F., et al. (2018). Structure and composition of rhodoliths from the Amazon River mouth. *Braz. J. South Am. Earth Sci.* 84, 149–159. doi: 10.1016/j.jsames.2018.03.014

Walbridge, S., Slocum, N., Pobuda, M., and Wright, D. J. (2018). Unified geomorphological analysis workflows with benthic terrain modeler. *Geosciences* 8:94. doi: 10.3390/geosciences8030094

Webster, J. M., Clague, D. A., Riker-Coleman, K., Gallup, C., Braga, J. C., Potts, D., et al. (2004). Drowning of the - 150 m reef off Hawaii: a casualty of global meltwater pulse 1A? *Geology* 32, 249–252. doi: 10.1130/G20170.1

Weiss, A. D. (2001). "Topographic position and landform analysis (poster)," in *Proceedings of the ESRI User Conference*, San Diego, CA.

Woodroffe, C. D., Brooke, B. P., Linklater, M., Kennedy, C., Jones, B. G., Buchanan, C., et al. (2010). Response of coral reefs to climate change: expansion and demise of the southernmost pacific coral reef. *Geophys. Res. Lett.* 37, 1–6. doi: 10.1029/2010GL044067

Conflict of Interest: The authors declare that the research was conducted in the absence of any commercial or financial relationships that could be construed as a potential conflict of interest.